# The effect of annealing on the conformational properties of xanthan hydrogels

**Francis X. Quinn* and Tatsuko Hatakeyama**
*Polymer Processing Laboratory, National Institute of Materials and Chemical Research, Tsukuba, Ibaraki 305, Japan*

**and Masato Takahashi**
*Department of Fine Materials Engineering, Faculty of Textile Science and Technology, Shinshu University, Ueda, Nagano 386, Japan*

**and Hyoe Hatakeyama**
*National Institute of Materials and Chemical Research, Tsukuba, Ibaraki 305, Japan*
*(Received 15 April 1993; revised 19 June 1993)*

Investigation of the nature of the freezing bound water in xanthan hydrogels by differential scanning calorimetry (d.s.c.) reveals a dependence of the area, temperature and number of the freezing exotherms on the period of time that the gel was maintained at a temperature greater than the gel–sol transition temperature ($T^*$). Small-angle X-ray scattering (SAXS) and synchrotron orbital radiation (SOR) experiments show a correlation between the holding time of the gel at temperatures in excess of $T^*$ and the size of the junction zones which maintain the integrity of the gel. High-temperature annealing also increases the elastic moduli of the gels. These results are discussed in terms of a general model for the dynamic structure of polysaccharide junction zones previously proposed by the authors.

**(Keywords: xanthan; hydrogel; junction zones)**

## INTRODUCTION

Xanthan gum is the generic name given to the anionic, extra-cellular polysaccharide produced by the bacterium *Xanthomonas campestris*. The chemical structure of xanthan is shown in *Figure 1*[1]. The physical and chemical properties of xanthan, and its commercial applications, are described in detail elsewhere[1]. In the solid state, in the presence of a nominal amount of water, xanthan adopts a double helical conformation[2,3]. Dilute solutions, above a threshold concentration (>0.5 wt%), form gels, the integrity of which are maintained by junction zones which are composed of oriented bundles of xanthan double helices. The junction zones are thought to be linked by extended helical chains, resulting in a three-dimensional network[4,5]. Various liquid-crystalline forms of xanthan have been reported over a wide range of water contents[6,7]. Xanthan gels exhibit a gel–sol transition in the region of 320 K, depending both on the concentration and $M_w$ of the xanthan used, and also on the nature of the cations present. The nature of the xanthan chains in the solution state has been widely discussed[8–15], the general consensus now being that semirigid (semiflexible), helical chains are present in solution.

In this study, which forms part of a general investigation into the gel structure of polysaccharide gels, differential scanning calorimetry (d.s.c.), thermomechanical analysis (t.m.a.) and small-angle X-ray scattering (SAXS) techniques are used to probe the dynamic structure of xanthan gels in the sol state in order to reveal its effect on the structure of the gel subsequently formed on cooling. Consequently, this work also examines the nature of the xanthan chains in the sol state and their ability to form aggregates when annealed.

## EXPERIMENTAL

### *Sample preparation*

Xanthan gum powder was received from the Mitsubishi Chemical Co., Ltd, and in order to investigate the effect of high-$M_w$ species on the gel structure the xanthan was used as supplied, without further purification. Aqueous stock solutions of xanthan were prepared using distilled, deionized water, and all glassware used in preparing the solutions was sterilized prior to use. Hermetically sealed solutions were placed in an oven, pre-heated to $313 \pm 0.5$ K, for 24 h. After this time the solutions were removed from the oven and cooled to room temperature; the condition of the gel after standing for one week was designated the initial state for all subsequent analysis. In this paper the solution concentration is given by the weight of xanthan powder (g) per 10 ml of water, expressed as a weight percentage. Thus, X(2.0) is equivalent to 0.2 g of xanthan

*To whom correspondence should be addressed

0032-3861/94/06/1248–05

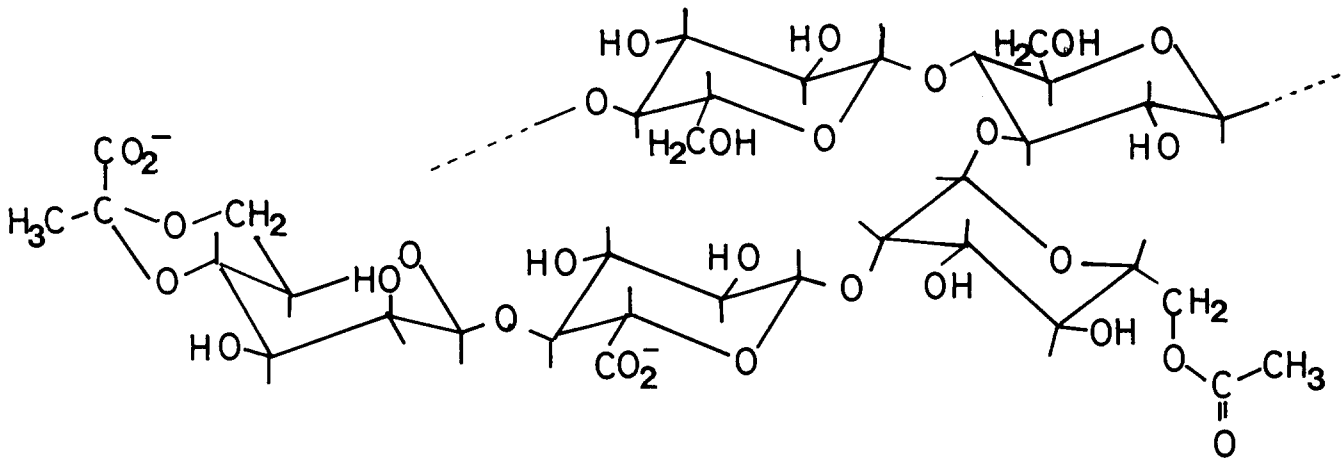

**Figure 1** The chemical structure of xanthan gum. The repeat unit consists of a linear backbone composed of (1→4)-β-D-glucose residues with a trisaccharide side group attached at atom C3 of every alternate glucose residue. The structure of the side group is as follows: the terminal β-D-mannose residue is glycosidically linked to the 4-poisiton of β-D-gluronic acid, which in turn is glycosidically linked to the 2-position of α-D-mannose

in 10 ml of water. The water content of the powder (as supplied) was taken into consideration when estimating the solution concentration. The solutions were not filtered at any stage during their preparation, and immediately after removing the samples from the preparation oven a visually clear solution was obtained in all cases.

*Thermal analysis*

A Perkin–Elmer DSC-2C differential scanning calorimeter, equipped with a low-temperature cooling apparatus, was used for all of the thermal analysis experiments. Temperature and energy calibrations were achieved using the crystal–crystal and melting transition peaks of spectroscopic grade cyclohexane. Samples were hermetically sealed in aluminium pans and scanned on both the heating and cooling cycles at a rate of 10 K $min^{-1}$. The sample weights varied between 4–5 mg, and no weight loss was recorded during the experiments.

*X-ray scattering analysis*

Small-angle X-ray scattering (SAXS) experiments were performed over the angular range $0° \leqslant 2\theta \leqslant 6°$ using a MAC Science Model MXP18 X-ray instrument, operating at 40 kV and 300 mA. The gel samples were irradiated with CuKα radiation of wavelength $\lambda = 0.154$ nm, at a constant sample temperature of $293 \pm 1$ K. Samples with a uniform thickness of 1 mm were sealed between poly(ether imide) sheets; no weight loss was recorded during the measurement time interval.

Synchrotron orbital radiation (SOR) experiments were carried out at the synchrotron facility of the National Laboratory for High Energy Physics, Tsukuba, Japan. The X-ray wavelength was selected using a double crystal monochrometer, and was fixed at $\lambda = 0.1488$ nm, for a constant sample temperature of $293 \pm 1$ K. A camera length of 2.0 m was used to examine the scattering profile, which was recorded using a unidirectional position sensitive proportional photon counter (PSPPC). The channel numbers of the PSPPC were cross-referenced with a standard collagen sample. As before, samples with a uniform thickness of 1 mm were sealed between poly(ether imide) sheets, with no weight loss was recorded during the measuring interval.

*Dynamic thermomechanical analysis*

The elastic modulus ($E'$) was measured at $298 \pm 0.2$ K by the needle penetration method, using a Seiko Instruments TMA-120. A uniform probe cross-sectional area (1 $mm^2$), operating frequency (0.05 Hz), load (5 mg) and probe penetration length (8.0 mm) were employed for all measurements to facilitate a comparison of the variation in $E'$ as a function of the gel concentration, holding temperature and holding time. The gel was covered with a layer of silicone oil (100 cs) to prevent evaporation from the gel during the measurements.

*pH measurements*

The pH of the xanthan gels was measured at 298 K by using a Horiba B-111 pH meter. The sensor was calibrated using standard solutions of neutral orthophosphate (pH = 6.8) and phthalic acid (pH = 4.0); measurements were reproducible to within ±0.1 pH.

## RESULTS

A sample of X(2.0) was placed in the differential scanning calorimeter, held at 365 K for 5 min, and then cooled to 130 K. A structured exotherm, exhibiting a small low-temperature feature, was observed on cooling. The freezing point was depressed by $\Delta T_m \approx 20$ K and the heat of fusion was considerably less than that of bulk water. Identical samples were held at 365 K for longer periods, and the recorded cooling curves are shown in *Figure 2a*. The structured exotherm observed after 5 min annealing is gradually replaced by two distinct peaks whose relative areas evolve with annealing time, as shown in *Figure 3*. In the case of the second exotherm $\Delta T_m \approx 25$ K. Following cooling the heating cycle was recorded. The sample that had been annealed for 5 min shows a large shoulder on the high-temperature side of the endotherm (see *Figure 2b*). This shoulder diminishes with annealing time, but the endotherm remains broad. Again, $\Delta H_{endo}$ is less than that of bulk water. The total area of the cooling cycle exotherm ($\Delta H_{exo}$) is plotted against the annealing time in *Figure 4*. At first, $\Delta H_{exo}$ increases, reaching a maximum after 15 min of annealing. Subsequently, $\Delta H_{exo}$ decreases linearly.

The scattering centres in the X-ray scattering

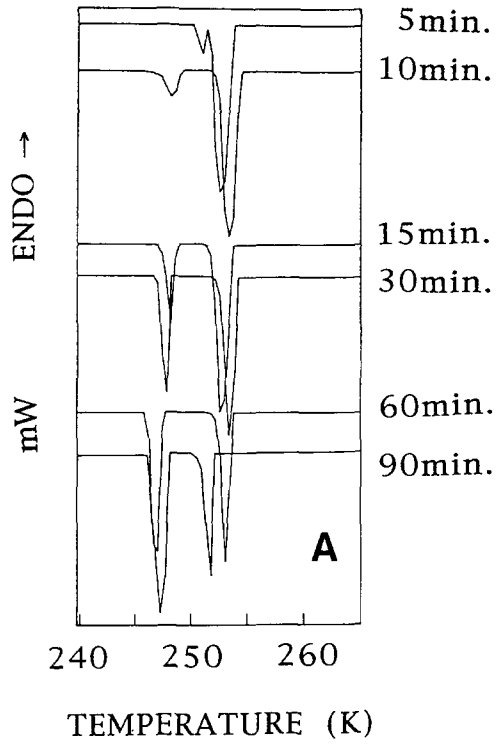


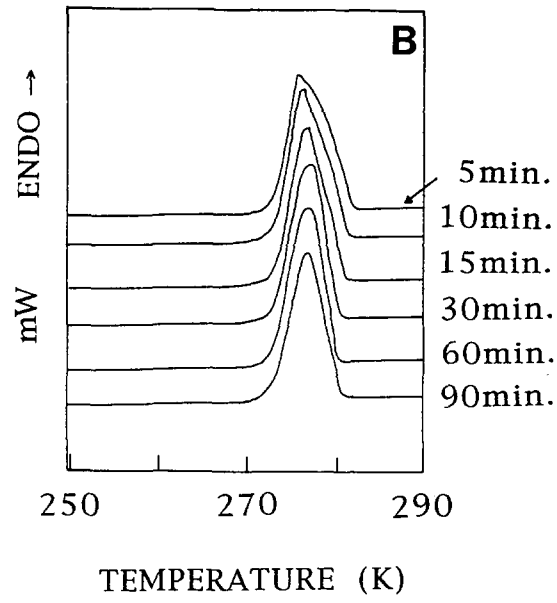


**Figure 2** Representative exotherms (A) and endotherms (B) for sample X(2.0) as a function of the annealing time at 365 K: rate = 10 K $min^{-1}$

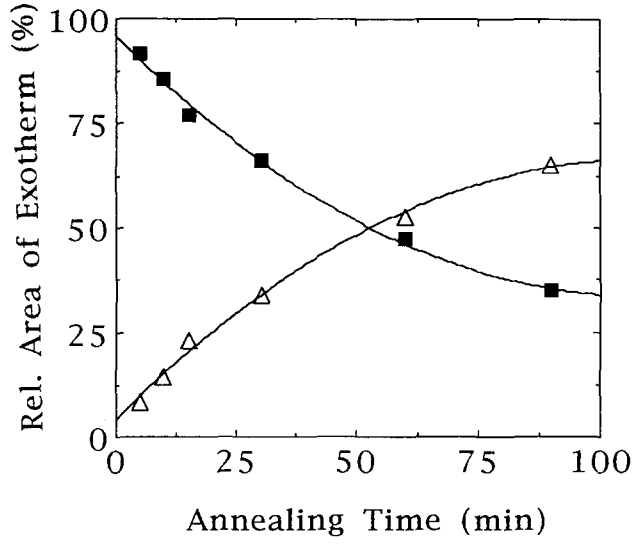


**Figure 3** Variation in the relative areas of the sample X(2.0) exotherms as a function of the annealing time at 365 K: (■) high-temperature peak and (△) low-temperature peak

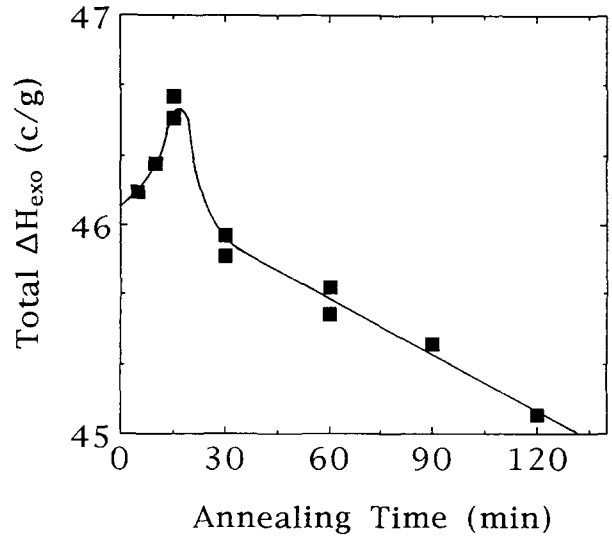


**Figure 4** The total area of the sample X(2.0) cooling exotherm ($\Delta H_{exo}$) as a function of the annealing time at 365 K

experiments are the junction zones in the gel which present themselves as ordered regions with random relative orientation and spatial distribution in the isotropic gel matrix[4]. SAXS analysis of X(2.0) revealed a diffraction peak in the region $0.1° \leqslant 2\theta \leqslant 0.4°$. The intensity of this peak, which can be related to a variation in the concentration of junction zones in the sample[4], showed a dependence on annealing time (see *Figure 5*). A peak was also observed in the SOR scattering profile of an identical sample, and is similarly ascribed to junction zones in the gel. Due to the high resolution of the SOR instrument a shift in the position of the peak, as a function of annealing time, was recorded and the results are summarized in *Figure 6*.

The variation in $E'$ of X(2.0) as a function of annealing time and annealing temperature was investigated, and the results are presented in *Figure 7*. At the two highest annealing temperatures a maximum in $E'$ is observed after approximately 60 min annealing. The subsequent decline in $E'$ may be caused by chain scission of the main chain or decomposition of the junction zones. The position of the maximum in $E'$ is inversely proportional to the holding temperature. The increase in the magnitude of $E'$ is strongly dependent on the annealing temperature and also on the solution concentration. *Figure 8* is a dual plot, which shows both the behaviour of $E'$ and the pH of X(2.0) gel, annealed at 365 K, as a function of annealing time. Clearly the molecular rearrangements responsible for the increase in $E'$ have direct implications for the pH of the gel. Such intrinsic changes in the pH of the gel with annealing may be caused by a change in the conformation of the trisaccharide side chain.

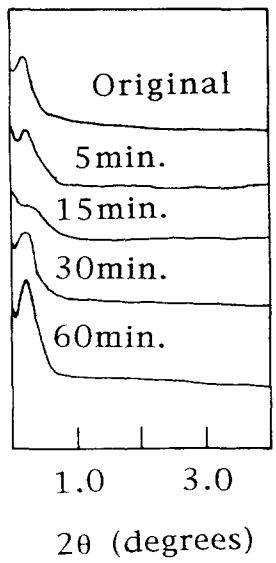


**Figure 5** The SAXS profile of the sample X(2.0) as a function of annealing time at 365 K; a diffraction peak is observed for $0.1° \leqslant 2\theta \leqslant 0.4°$. All profiles are plotted on the same vertical and horizontal scales

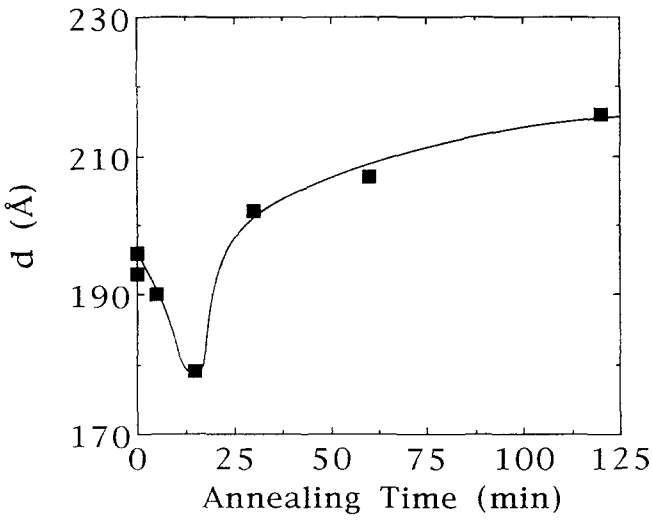


**Figure 6** The position of the maximum of the SOR scattering peak as a function of annealing time at 365 K for the sample X(2.0)

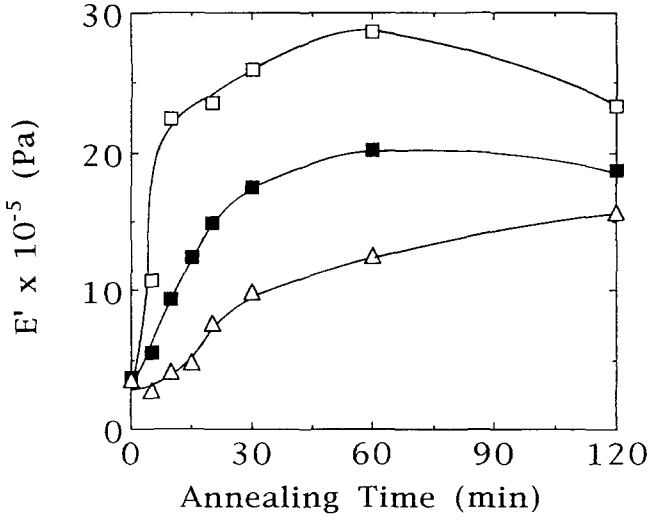


**Figure 7** The variation in the elastic modulus ($E'$) with annealing time measured at various temperatures for the sample X(2.0): (□) 365; (■) 350 and (△) 340 K

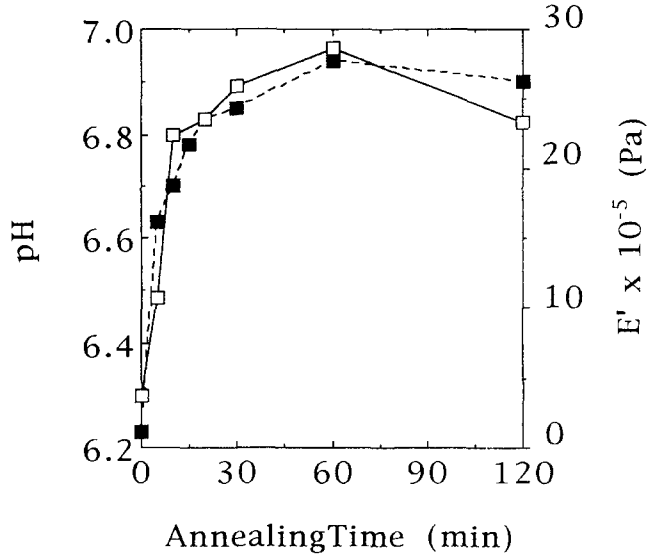


**Figure 8** A dual plot showing the variation in $E'$ (□) and pH (■) with annealing time measured at 365 K for the sample X(2.0)

## DISCUSSION

The results cited above demonstrate that molecular restructuring in the xanthan gel system at temperatures greater than $T^*$ has a profound effect on the properties of the gel that is subsequently formed on cooling. D.s.c. analysis reveals that with increased annealing the freezing bound water in the system gradually enters a more coordinated state, as indicated by the development of a second lower-temperature exotherm (with a concomitant decrease in the area of the high-temperature exotherm) and a reduction in $\Delta H_{exo}$. The heating cycle data also show a dependence on the annealing time. However, due to the width of the endotherm, $\Delta H_{endo}$ was found to be constant within a large experimental error. An increase in the degree of association between the water and polysaccharide phases suggests that a higher-order structure may evolve during the annealing process[4]. The behaviour of $\Delta H_{exo}$ compares favourably with the X-ray data. The initial increase in $\Delta H_{exo}$, which reaches a maximum after 15 min, coincides with the minimum in the SAXS diffraction peak intensity and the minimum in the size of the junction zones.

Small-angle X-ray scattering is observed from any system which possesses heterogeneities on the appropriate distance scale and is not therefore solely confined to well defined particles. For a system consisting of two components, with individual, constant electron densities, by Babinet's principle it is impossible to unambiguously assign the distance parameter calculated from the position of the diffraction peak to either component on the basis of the X-ray analysis alone. In xanthan hydrogels the position of the maximum of the SAXS diffraction peak, $d$, can correspond to either the average size of the scattering centres in the gel, or to the mean inter-scattering centre distance (i.e. the mean mesh size). Complementary experiments were carried out in an attempt to resolve this problem, and thereby to correctly interpret the SAXS results.

It is proposed that $d$ be taken to represent the average size of the scattering centres in the gel, in this case the junction zones. The initial decrease in $d$, observed for annealing times up to 15 min at 365 K, represents a partial denaturation of xanthan, where primarily the junction

zones are disrupted, thereby reducing their average size. This results in a decrease in the intensity of the SAXS peak as the effective concentration of scattering centres in the system is reduced. Disruption of the junction zones means that the amount of water molecules in close association with the polysaccharide matrix (including freezing bound water) is reduced and so the overall water behaviour becomes more bulk-like. This partial denaturation should not be viewed as a widespread unravelling of the xanthan double helix. In the solution state there exists, at this stage, a small number of junction zones still relatively unperturbed, as well as double helices with various degrees of helical character and extended helix single chains.

On annealing for longer periods (>30 min) the average size of the junction zones increases to values greater than in the unannealed state and the following observations are made: (i) the freezing bound water is more coordinated with the xanthan matrix, (ii) the intensity of the SAXS diffraction peak, and therefore the concentration of scattering centres, has recovered, and actually surpassed the unannealed value, and (iii) the elastic modulus has increased considerably. These observations are consistent with the hypothesis that $d$ represents the average junction zone size. The sol state in this case cannot be considered as an isotropic liquid state, but rather a high-order structure is formed, leading to the observed experimental behaviour. The existence, in the sol state, of double helices and individual polysaccharide chains participating in the formation of a high-order structure has been proposed[16], and inferred experimentally, in DNA and collagen[17,18]. A similar situation may occur here where the relatively unperturbed junction zones act to nucleate aggregation. The reduction in entropy caused by aggregation is offset by the contribution from the configurational entropy and configurational degeneracy of the large agglomerated polysaccharide chains. The presence of the highest-molecular-weight fraction of the polysaccharide in the solution is crucial if there is to be an overall increase in the entropy of the system as the aggregation proceeds[16]. It is probable that the large-scale side chain mobility, which occurs before an increase in backbone mobility is observed[19], plays an important role in controlling the conformation of the xanthan double helices in the aggregates. Further evidence for the pre-eminent role of the trisaccharide side chain in aggregate formation comes from the close correspondence between pH and $E'$ and the observed changes in the environment of the acetate group above $T^*$ [13]. Structure formation in the solution state during annealing is inferred from the following observations: (i) the recovery of the intensity of the SAXS diffraction peak after annealing, (ii) the linear decrease in $\Delta H_{exo}$, which is observed as the freezing bound water becomes more tightly bound in the aggregates, (iii) the increase in $E'$ of the cooled gels, (iv) the observation of a liquid-crystalline type structure in the samples, and (v) the displacement of the SOR peak to larger values of $d$.

Prolonged annealing results in an eventual decrease in $E'$, and a reduction in the junction zone concentration and size. These effects are probably caused by acid hydrolysis induced main-chain scission and/or decomposition of the junction zones. This decomposition leads to a permanent denaturation of the xanthan gum.

Alternatively, $d$ may be taken to represent the mean mesh size of the hydrogel, but as the following consideration of the collated results reveals, this assumption leads to contradictory behaviour in the system. After 15 min annealing at 365 K the mean mesh size decreases. However, following identical annealing conditions, d.s.c. analysis reveals that the freezing bound water is in a less associated state with the xanthan matrix and that the environment of this water fraction is more bulk-like. Also, the intensity of the SAXS diffraction peak decreases after 15 min annealing at this temperature, indicating that the concentration of the scattering centres has decreased as a result of the annealing process. For longer annealing times (>30 min) at 365 K the value of $d$ has recovered, actually exceeding the value of the unannealed gel, and this would correspond to an increase in the mean mesh size. In contrast, under these annealing conditions the freezing bound water in the gel has entered a more associated state with the polysaccharide matrix ($\Delta H_{exo}$ is less than the unannealed or the 15 min annealed value) and the elastic modulus of the gel has increased considerably. Furthermore, the concentration of scattering centres has recovered and a liquid-crystalline type structure is observed in the hydrogel. Therefore, for both short annealing times (where $d$ is a minimum) and also longer annealing times (where $d$ is greater than in the unannealed state) consideration of $d$ as representing the average mesh size of the gel is not in accordance with the other experimental observations.

## CONCLUSION

D.s.c., t.m.a., and small-angle X-ray scattering analyses reveal that the sol state of xanthan hydrogels is not an isotropic liquid state, but that, in fact, a high-order structure is developed in solution as the result of annealing. This high-temperature annealing leads to an increase in the size of the junction zones and the elastic moduli of the gels that are subsequently formed on cooling.

## REFERENCES


1 'Handbook of Water-Soluble Gums and Resins' (Ed. R. L. Davidson), McGraw-Hill, New York, 1980
2 Okuyama, K., Arnott, S., Moorhouse, R., Walkinshaw, M. D., Atkins, E. D. T. and Wolf-Ullish, C. in 'Fiber Diffraction Methods' (Eds A. D. French and K. H. Gardner), American Chemical Society, Washington, DC, 1980, p. 411
3 Moorhouse, R., Walkinshaw, M. D., Winter, W. T. and Arnott, S. in 'Cellulose Chemistry and Technology' (Ed. J. C. Arthur), American Chemical Society, Washington, DC, 1977, p. ?
4 Quinn, F. X., Hatakeyama, T., Yoshida, H., Takahashi, M. and Hatakeyama, H. *Polym. Gels Networks* 1993, **1**, 45
5 Southwick, J. G., Jamieson, A. M. and Blackwell, J. *Macromolecules* 1981, **14**, 1728
6 Maret, G., Milas, M. and Rinaudo, M. *Polym. Bull.* 1981, **4**, 291
7 Yoshida, H., Hatakeyama, T. and Hatakeyama, H. *Polymer* 1990, **31**, 693
8 Hacche, L. S., Washington, G. E. and Brant, D. A. *Macromolecules* 1987, **20**, 2179
9 Sato, T., Norisuye, T. and Fujita, H. *Polym. J.* 1984, **16**, 341
10 Sato, T., Norisuye, T. and Fujita, H. *Polym. J.* 1984, **16**, 423
11 Paradossi, G. and Brant, D. A. *Macromolecules* 1982, **15**, 874
12 Oertel, R. and Kulicke, W.-M. *Rheol. Acta* 1991, **30**, 140
13 Southwick, J. G., McDonnell, M. E., Jamieson, A. M. and Blackwell, J. *Macromolecules* 1979, **12**, 305
14 Muller, G., Lecourtier, J., Chauveteau, G. and Allain, C. *Makromol. Chem. Rapid Commun.* 1984, **5**, 203
15 Ross-Murphy, S. B., Morris, V. J. and Morris, E. R. *Faraday Symp. Chem. Soc.* 1983, **18**, 115
16 Shibata, J. H. and Schurr, J. M. *Biopolymers* 1981, **20**, 525
17 Elson, E. L. and Record, M. T. *Biopolymers* 1974, **13**, 797
18 Kallay, M. and Record, M. T. *Biopolymers* 1974, **13**, 825
19 Gamini, A., de Bleijser, J. and Leyte, J. C. *Carbohydr. Res.* 1991, **220**, 33